The Mach-Zehnder interferometer: examination of a volume by non-classical localization plane shifting

2001 J. Opt. A: Pure Appl. Opt. 3 242

(http://iopscience.iop.org/1464-4258/3/4/303)

INSTITUTE OF PHYSICS PUBLISHING JOURNAL OF OPTICS A: PURE AND APPLIED OPTICS

J. Opt. A: Pure Appl. Opt. **3** (2001) 242–249 www.iop.org/Journals/oa PII: S1464-4258(01)19592-9

The Mach–Zehnder interferometer: examination of a volume by non-classical localization plane shifting

Juan M Simon[1], **Silvia A Comastri**[1,2] **and Rodolfo M Echarri**[1,2]

[1] Universidad de Buenos Aires, Facultad de Ciencias Exactas y Naturales, Laboratorio de Optica, Departamento de Fisica, Ciudad Universitaria, Pabellón I (1428) Nuñez, Buenos Aires, Argentina

[2] Consejo Nacional de Investigaciones Cientificas y Técnicas

E-mail: simon@df.uba.ar, comastri@df.uba.ar and tgre@df.uba.ar

Received 30 October 2000, in final form 21 March 2001

Abstract

The Mach–Zehnder interferometer can be used as is customary in optical testing but, to examine different layers of a volume, the procedure of either readjusting the interferometer or displacing the specimen can be avoided, employing an incoherent periodic source. In this case, leaving the specimen in a fixed position and without readjusting the interferometer, the different layers can be analysed, shifting a non-classical localization plane by a change in the source period. In this paper experimental interferograms, obtained by varying this period to map the disturbances present on either one or both faces of a phase object, are shown.

Keywords: Interferometry, transparent media exploration

1. Introduction

The Mach–Zehnder is the basic interferometer for measurements of phase variations across a field in single passage [1]; it is more versatile than common path interferometers but more complicated to align [2] and usually has more requirements concerning mechanical stability. The conventional Mach–Zehnder interferometer is composed by two plane mirrors and two partially reflecting beam splitters with one surface often coated with a metal and the other sometimes coated with an anti-reflector to avoid multiple reflections. If each component is separately mounted on a suitable base, the mirrors or beam splitters can be given a rotation about an axis normal to the plane of the instrument to introduce shear and tilt independently without introducing shift or lead. There are two accessible interferograms, the first viewed in a direction parallel to that of the incident beam and the second perpendicular to it, but the latter is seldom used in optical testing because small differences between the reflectivity and transmissivity of the beam splitters result in a faint pattern.

Hariharan [3] has introduced a modification of the Mach–Zehnder replacing the mirrors by pentaprisms to achieve an easier adjustment and allow for non-complicated displacements of the classical localization plane. However the method we propose does not require readjustments of the interferometer. We take into account the conventional Mach–Zehnder, regarding it as a plane instrument [1] with two arms and consider the interferogram viewed in a direction parallel to that of the incident beam. The specimen to be tested is a phase object with defects distributed in its volume and the defects present in a layer can be determined by measuring the departures from straightness of the fringes viewed on an adequate observation plane.

One of the fundamental choices in the design of the interferometer is the source to be used. As is known [1], if an expanded laser is employed, the need for matching the arms disappears, the spectral bandwidth is narrow, the source is small and of large spatial coherence and the density of energy is high. However the coherence length is so large that interference takes place between the two main beams and all the other beams reflected from surfaces of optical components and, since none of the fringes are localized, unwanted fringes appear superimposed on those due to the interference of the two main beams. To reduce these inconveniences an extended incoherent source is frequently used so fringes are seen on the localization surfaces and the spatial coherence in other places is low. In the particular case in which the incoherent source consists of an expanded laser beam incident on a rapidly rotating diffusor [1, 4, 5], the spatial coherence is suppressed while the temporal coherence is preserved and high enough for the matching of the arms to be unnecessary. When the source is continuous, the test fringes can be seen only on the classical localization plane provided this plane exists, this is if a ray incident on the interferometer splits into two rays that remain in the same plane [1, 6–8]. In a conventional Mach–Zehnder this surface can be shifted modifying the tilt and it can be either virtual or real. To test a volume under these circumstances either the specimen or the classical localization surface has to be shifted. The first alternative may be troublesome or even practically impossible, for example if the specimen is part of a larger equipment or if it is fluid, while the second has the disadvantage of having to revise the adjustment of the instrument to test each layer. These drawbacks can be overcome by the employment of an incoherent periodic source. In this case localization planes of different orders m appear on both sides of the classical localization one (which corresponds to $m = 0$) and we have given [9–11] analytical expressions for the position, fringe spacing, contrast and fringe localization depth of these localization planes. This type of source has also been used when the interferometer is a grating [12] though not to examine a volume. In two beam interferometers such a source can be used in optical testing and recently we have considered [13] where we consider a Wollaston prism, which is an interferometer more easily aligned than the Mach–Zehnder but has the disadvantages that it is less versatile, the disturbance present in the phase object appears in both arms and the measurements can be more complicated. The method we propose to test different layers of a phase object is very simple. We illuminate the interferometer with a periodic source, we focus the observation optical system to view a layer and we shift a non-classical localization plane until fringes of adequate contrast are seen. Thus we profit from the relation between the position of a non-classical localization plane and the source period to employ such a plane in measurements of phase variations across a volume.

The phenomenon of multiple localization in a Mach-Zehnder, together with a procedure of alignment that allows the different localization planes to be viewed without readjusting the interferometer, have been considered in another paper [14]. The present article complements the former one, since we show how this interferometer can be used to test a volume. In section 2 we summarize the basic formulae of the general theory of multilocalization, we give a brief review of the theory underlying the method we propose to examine a phase object and we apply this method to the Mach–Zehnder. In section 3 we present two experiments that corroborate qualitatively the theory developed and make evident some of the limitations of the phase objects that can be analysed. In the appendix, for completeness, we explain the procedure of alignment previously given.

2. Optical testing with a Mach–Zehnder

An amplitude division interferometer with a specimen inside it records the phase shifts introduced and can yield information concerning surface irregularities or variation of refractive index. For a two-beam interferometer illuminated by a source, σ, emitting quasi-monochromatic radiation of mean wavelength in vacuum $\bar{\lambda}$, we define [10, 11, 13] an orthogonal coordinate system (x, y, z) with origin at the central source point, O, and (x, y) on the source plane (figures 1(a) and (b)). We assume there is translational symmetry along the y-axis and that there are negligible equivalent aberrations except for those introduced by the specimen. If the two arms are labelled I and II, the images of σ and O through arm I (or II) are termed σ' and O$'$ (or σ'' and O$''$) respectively and σ, σ' and σ'' have sizes $2H$, $2H'$ and $2H''$ along x. A ray from O which subtends an angle β_{II} with z, splits into two rays, 'I' and 'II', which intersect at a point $\mathrm{P}'_{\mathrm{loc}}$ of the classical localization surface, Σ'_0, and the images of $\mathrm{P}'_{\mathrm{loc}}$ back through arms I and II are termed $\mathrm{P}_{\mathrm{I,loc}}$ and $\mathrm{P}_{\mathrm{II,loc}}$. Another ray from O, OP_{I}, subtends an angle β_{I} with z and gives rise through arm I to a ray '$\tilde{I}$', which intersects 'II' at a point P$'$ of an arbitrary observation plane, Σ'. The optical pathlengths from a source point S_k of coordinates (x, y) to P$'$ along arms I and II are labelled $[\mathrm{S}_k\mathrm{P}']_{\mathrm{I}}$ and $[\mathrm{S}_k\mathrm{P}']_{\mathrm{II}}$ and the difference $[\mathrm{S}_k\mathrm{P}']_{\mathrm{I}} - [\mathrm{S}_k\mathrm{P}']_{\mathrm{II}}$ is assumed to be less than the coherence length. The variation of optical pathlength difference at P$'$ is [10]

$$\begin{aligned}\mathrm{VOPD}(\mathrm{P}') &= [\mathrm{S}_k\mathrm{P}']_{\mathrm{I}} - [\mathrm{S}_k\mathrm{P}']_{\mathrm{II}} - [\mathrm{OP}']_{\mathrm{I}} + [\mathrm{OP}']_{\mathrm{II}} \\ &= [\mathrm{S}_k\mathrm{P}_{\mathrm{I}}] - [\mathrm{S}_k\mathrm{P}_{\mathrm{II}}] - [\mathrm{OP}_{\mathrm{I}}] + [\mathrm{OP}_{\mathrm{II}}] \qquad (1)\end{aligned}$$

where square brackets indicate optical pathlength; P_{I} and P_{II} are the images of P$'$ back through arms I and II and $p_{\mathrm{I}} = [\mathrm{P}_{\mathrm{I}}\mathrm{P}']$ and $p_{\mathrm{II}} = [\mathrm{P}_{\mathrm{II}}\mathrm{P}']$ are independent of (x, y). If the two beams leave the interferometer in the same state of polarization, the intensity is

$$\begin{aligned}I(\mathrm{P}') = {} & I^{(\mathrm{I})}(\mathrm{P}') + I^{(\mathrm{II})}(\mathrm{P}') + 2\sqrt{I^{(\mathrm{I})}(\mathrm{P}')I^{(\mathrm{II})}(\mathrm{P}')} \\ & \times|\mu_{\mathrm{I,II}}(\mathrm{P}')|\cos(\Psi(\mathrm{P}')) \qquad (2)\end{aligned}$$

$\Psi(\mathrm{P}')$ being the phase difference, defined as

$$\Psi(\mathrm{P}') = \arg(\mu_{\mathrm{I,II}}(\mathrm{P}')) + \gamma_{\mathrm{I,II}} - \frac{2\pi}{\bar{\lambda}}([\mathrm{OP}']_{\mathrm{II}} - [\mathrm{OP}']_{\mathrm{I}}) \qquad (3)$$

where $\mu_{\mathrm{I,II}}(\mathrm{P}') = |\mu_{\mathrm{I,II}}(\mathrm{P}')|\exp(\mathrm{i}\arg\mu_{\mathrm{I,II}}(\mathrm{P}'))$ is the degree of coherence and $\gamma_{\mathrm{I,II}} = \gamma_{\mathrm{I}} - \gamma_{\mathrm{II}}$ (γ_{I} and γ_{II} take into account the phase shifts of the portion of the light travelling through arms I and II). If the source consists in a periodic array of N incoherent sources parallel to the y-axis, each of width b, and if δx is the source period, there are localization planes, denoted Σ'_m, of different orders m (m integer) which verify that the variation of optical pathlength difference for two consecutive sources is $\mathrm{VOPD}(\mathrm{P}')|_{\delta x} = -m\bar{\lambda}$. In terms of variables of the source and observation spaces, these planes are such that [10]

$$\begin{aligned}\sin\beta_{\mathrm{I}m} - \sin\beta_{\mathrm{II}m} &= \frac{m\bar{\lambda}}{n\delta x} \\ Z''_m = \frac{F'm\varepsilon^{(0)}}{q_1\delta x - m\varepsilon^{(0)}} &= \frac{F'}{(q_1\delta x|\Lambda'|/m\bar{\lambda}) - 1}\end{aligned} \qquad (4)$$

where, if the medium of the observation space is air and the angle β'_{II} from the normal to σ' to ray $\mathrm{O}'\mathrm{P}'_{\mathrm{loc}}$ is small, we have

$$\begin{aligned}F' &= \mathrm{O}'\mathrm{P}'_{\mathrm{loc}} \qquad & Z'' &= \mathrm{P}'_{\mathrm{loc}}\mathrm{P}' \\ \varepsilon^{(0)} &= \frac{\bar{\lambda}}{|\Lambda'|} \qquad & q_1 &\approx \frac{H'}{H}\end{aligned} \qquad (5)$$

$\varepsilon^{(0)}$ being the fringe spacing at Σ'_0 (Λ' is the angle from 'II' to 'I') and q_1 being equal to one for unitary magnification through arm I. In equation (4) we see that for a given setup (i.e. if F',

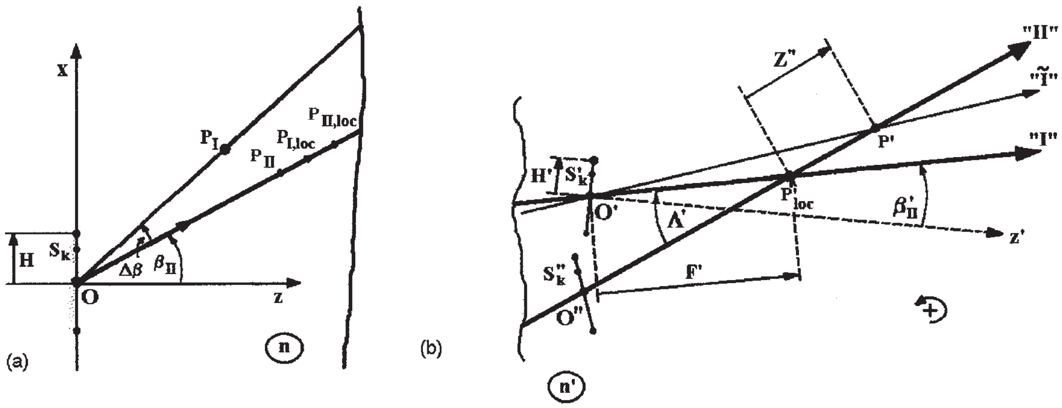

Figure 1. Amplitude division interferometer: P'_{loc} (or P'), point at the classical localization (or at any observation) plane where the rays 'II' and 'I' (or 'Ĩ') intersect; $P_{I,loc}$ and $P_{II,loc}$ (or P_I and P_{II}), images of P'_{loc} (or P') by inverse ray tracing. (*a*) Source space: O (or S_k), central (or any) source point; (x, y, z), orthogonal coordinates (z normal to the source); β_{II} (and $\beta_I = \beta_{II} + \Delta\beta$), angles from the z-axis to rays OP_{II} (and OP_I); n, refractive index. (*b*) Observation space: O' and O'', images of O through both arms; z', normal to the source image through arm I; Z'', distance from P'_{loc} to P'; β'_{II}, angle from z' to ray $O'P'_{loc}$, $F' = O'P'_{loc}$; Λ', angle from ray 'II' to 'I'; n', refractive index.

Λ', q_1 and $\bar{\lambda}$ are fixed), the location of plane Σ'_m depends on m and on δx. From equation (37) of [10], the fringe spacing at Σ'_m is

$$\varepsilon^{(m)} \approx \varepsilon^{(0)}\left(1 + \frac{Z''_m}{F'}\right) = \frac{\varepsilon^{(0)}}{1 - m\varepsilon^{(0)}/(q_1\delta x)} \qquad (6)$$

so that if $m < 0$ then $Z''_m < 0$ and $\varepsilon^{(m)} < \varepsilon^{(0)}$ (to maintain the notation of former papers [10, 13], we here use a notation different from that of [14] and F', Z'', $\varepsilon^{(0)}$, Λ', β_I and β_{II} represent h_s, $-h_m$, Δ_o, β, θ_1 and θ_2 respectively). Furthermore, according to equation (39) of [10], the localization depth, $LD^+|_m$, can be calculated as the distance from Σ'_m to the first zero of visibility on the right of Σ'_m (similarly $LD^-|_m$ on the left). Writing $LD^+|_m$ not only as in [10], but also as a function of $2H = N\delta x$, $\varepsilon^{(m)}$ and $(F'+Z''_m)$,

$$\begin{aligned} LD^+|_m &= Z''_{m+1/N} - Z''_m \\ &= \frac{F' q_1 \delta x}{\varepsilon^{(0)}(q_1\delta x/\varepsilon^{(0)} - m)(N(q_1\delta x/\varepsilon^{(0)} - m) - 1)} \\ &= \frac{(F' + Z''_m)\varepsilon^{(m)}}{2Hq_1(1 - \varepsilon^{(m)}/(2Hq_1))} \end{aligned} \qquad (7)$$

so if $m < 0$ then $LD^+|_m < LD^+|_{m=0}$. Though in equation (7) $LD^+|_m$ is independent of the slit width, in practical applications the region around Σ'_m where fringes are seen is smaller than $LD^+|_m$ and the exact value depends on the contrast on Σ_m (which depends on b).

In this paper we are concerned with the employment of a Mach–Zehnder interferometer to examine a specimen with a few phase disturbances distributed in its volume. Before placing the phase object, the interferometer is aligned using the procedure previously described [14], which, for the sake of completeness, we rewrite in the appendix. The illumination optical system (IS) renders an effective source σ and the observation system (OS) is used to view the observation planes (figure 2(*a*)). There are two identical semitransparent beam splitters, BS_1 and BS_2, and two mirrors, M_I and M_{II}, and all the surfaces are plane so $H = H' = H''$. In arm II, hereinafter considered the test arm, O''_{i1} is the image of O by reflection on BS_1; O''_{i2} is the image of O''_{i1} by reflection on M_{II} and O'' is the image of O''_{i2} by refraction in BS_2. In arm I, which from now on is the reference arm, O'_{i1} is the image of O by refraction in BS_1; O'_{i2} is the image of O'_{i1} by reflection on M_I and O' is the image of O'_{i2} by reflection on BS_2. The ray from O which is along z splits into two rays, 'II_o' and 'I_o', which intersect at a point $P'_{loc,o}$ forming a small bifurcation angle, Λ'_o. Rays 'I_o' and 'II_o' intersect an arbitrary plane Σ' at points B' and B'' respectively and we assume that the lead can be neglected; the tilt is $t'_o = O'O''$ and the shear is lateral and, in the observation representation, it is $s'_o = B'B''$ [1, 13].

When the alignment procedure is completed, the specimen is introduced into the test arm. To examine the layer which is viewed on a plane that we denote Σ'_M we consider that, for the interferogram to map the disturbance at the layer, the observation system must focus plane Σ'_M and, for the contrast to be adequate, the source period must be such that Σ'_M is a localization plane [13]. The first requirement can be understood taking into account the light originating at O and considering that the spherical wavefront emerging from O'' is distorted as it passes through the phase object; when it immediately leaves the layer under consideration, it maps the disturbances present there but, as it propagates, its shape varies (figure 2(*b*)). The second requirement is encountered considering all the source points since at plane Σ'_M the wavefronts originating at different points of σ'' are distorted in approximately the same region and in a similar way and, additionally, the contrast is adequate only if Σ'_M is a localization plane. The disturbance can be evaluated, considering at Σ'_M a coordinate system (ξ', η') parallel to (x, y); defining the deformation of the wavefront, $w''(\xi', \eta')$, as the optical pathlength from the ideal sphere originating at O'' to the real wavefront and defining

$$\Psi^{(\sigma)} = \arg(\mu_{I,\,II}(P')) + \gamma_{I,\,II} - \frac{2\pi}{\bar{\lambda}}([OO''] - [OO']) \qquad (8)$$

which is locally independent of P' because the constant contrast condition [10] is assumed to hold. From equations (3) and (8), the phase difference at a point of coordinates (ξ', η') is

$$\Psi(\xi', \eta') = \Psi^{(\sigma)} + \frac{2\pi}{\varepsilon^{(M)}}\xi' + \frac{2\pi}{\bar{\lambda}} w''(\xi', \eta') \qquad (9)$$

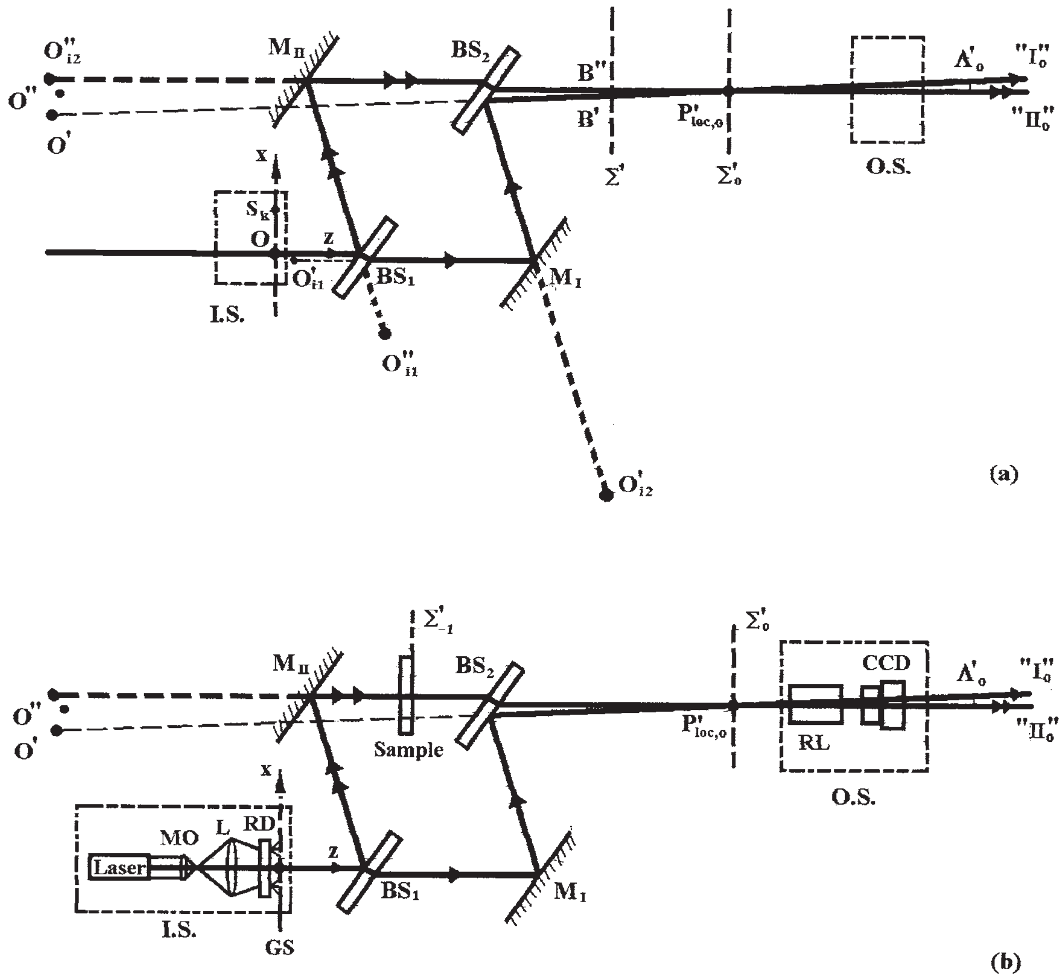

Figure 2. Mach–Zehnder interferometer: IS, illumination optical system; OS, observation optical system; BS_1 and BS_2, beam splitters; M_I and M_{II}, mirrors; O (and S_k), central (and other) source point; $P'_{loc,o}$, intersection of rays 'I_o' and 'II_o' originated when the ray along z splits; Λ'_o, bifurcation angle. (*a*) B' and B'': points where rays 'I_o' and 'II_o' intersect an arbitrary observation surface Σ'. (*b*) IS consists of a laser, a microscope objective (MO), a condenser (L), a rotating diffusor (RD) and a set of gratings (GS); OS consists of a relay lens (RL) and a CCD camera with objective and approximation lens.

so, if ξ'_J and ξ'_{0J} (with J integer) are the coordinates for the Jth bright fringe in the presence and absence of disturbances respectively (i.e. $\Psi(\xi'_J, \eta'_J) = \Psi(\xi'_{0J}, \eta'_{0J}) = 2\pi J$),

$$w''(\xi'_J, \eta'_J) = \bar{\lambda}\frac{\xi'_{0J} - \xi'_J}{\varepsilon^{(M)}} \tag{10}$$

where $\varepsilon^{(M)}$ is the fringe spacing at plane Σ'_M. Thus, as is known [1], a displacement of fringes equal to $\varepsilon^{(M)}$ means that the deformation of the wavefront is equal to $\bar{\lambda}$. Counting the number of displaced fringes, $(\xi'_{0J} - \xi'_J)/\varepsilon^{(M)}$, the deformation of the wavefront and, consequently, the disturbance at the layer can be determined. There are several highly precise methods for automatically analysing the fringes, e.g. [1, 15, 16], but the description of these methods is beyond the aim of this paper.

To test different layers, since the positions of the planes Σ'_m with $m \neq 0$ depend on δx (see equation (4)), a non-classical localization plane is made to coincide with a layer and is then shifted by varying the source period. Therefore to examine a volume, we do not need either to displace the specimen or to readjust the interferometer.

3. Experiments

The interferometer is mounted on an holographic table so that vibrations are minimized. The beam splitters are made in our laboratory in such a way that the surface of a glass plate which is going to reflect the beam is coated with aluminium; the beam reflected from the other surface can be neglected and the interferometer can be considered to have only two arms. As explained in the appendix, the illumination system (IS) varies in the different steps of the alignment procedure though we always use laser illumination, diffuse or not, to obtain large tolerances regarding the difference in arm lengths. We use a polarized He–Ne laser ($\bar{\lambda} = 0.6328$ μm and exit power 7 mW) and the emerging beam is linearly polarized perpendicular to the plane of the interferometer. Our practical setup is that of figure 2(*a*), the Mach–Zehnder is mounted in rhomboidal configuration and the lengths of the arms differ by less than 10 mm (so the lead is small). Giving to the beam splitters and mirrors a rotation about an axis normal to the plane of the instrument, the classical localization surface is placed 10 mm to the right of BS_2, the bifurcation angle (determined during step 1 of the alignment procedure) is $\Lambda'_{\mathrm{o}} = 1.79^{\circ}$ and the distance from O′ to Σ'_0 is $F' \approx 500$ mm.

When the interferograms needed to test a specimen are acquired, the IS is that of figure 2(*b*) and consists of the laser, a microscope objective (MO), a condenser (L), a rotating diffusor (RD) and a set of gratings of different periods (GS). The set we use is produced in our laboratory, drawing the gratings with a PC program, printing them from the PC and reducing the images by a factor of six to impress them on a microfilm. The set is placed approximately 3 mm away from the rotating diffusor, while the microscope objective and the condenser allow an adequate extension of this diffusor to be illuminated. The observation optical system (OS) slides along an optical bench parallel to ray '$\mathrm{II_o}$', which, since Λ'_{o} is small, is approximately perpendicular to the localization planes. The OS consists of a relay lens (RL), used to increase the range of observation planes accessible to the CCD camera, and a CCD Sony 95C with a 50 mm objective and a 8 mm approximation lens that captures a field of approximately 1.5 mm. The images acquired by the CCD are recorded averaging 256 TV images to diminish the noise present and they are later adjusted and printed with an image processing program.

The phase object consists of a plane parallel plate approximately 10 mm thick of float glass (refractive index $n_{\mathrm{g}} \approx 1.5$) with one or two thin Mylar strips (refractive index $n_{\mathrm{M}} \approx 1.5$) adhered by the electrostatic effect generated by friction. We carry out the two following experiments.

3.1. Experiment 1: the disturbance is on one face of the specimen

A glass plate with a Mylar strip adhered to one of its faces is placed in the test arm with the border of the strip inclined at approximately 45° to the x-axis. We take into account six gratings of periods

$$\begin{array}{lll} \delta x_1 = 0.239 \text{ mm} & \delta x_2 = 0.217 \text{ mm} & \delta x_3 = 0.195 \text{ mm} \\ \delta x_4 = 0.174 \text{ mm} & \delta x_5 = 0.152 \text{ mm} & \delta x_6 = 0.130 \text{ mm}. \end{array} \tag{11}$$

The localization plane of order $m = -1$ corresponding to the grating of period δx_k is termed $\Sigma'_{-1}|_k$ (with $k = 1, \ldots, 6$) and, since $\delta x_1 \geqslant \delta x_k$, $\Sigma'_{-1}|_k$ is to the left of $\Sigma'_{-1}|_1$ (see equation (4)). The face of the specimen containing the disturbance is focused with the observation system; the Mylar strip is seen on the left upper corner of the image; the grating which yields the localization surface of order $m = -1$ on this face turns out to be that of period δx_4 and plane $\Sigma'_{-1}|_4$ is approximately 53 mm to the left of Σ'_0. In figure 3 we show images acquired at the planes (*a*) $\Sigma'_{-1}|_6$, (*b*) $\Sigma'_{-1}|_4$, (*c*) $\Sigma'_{-1}|_2$ and (*d*) Σ'_0. Since the image of figure 3(*b*) is on the plane $\Sigma'_{-1}|_4$, which coincides with the face of the plate containing the strip, the deformation of the wavefront in the test arm is $w''(\xi'_J, \eta'_J) = \bar{\lambda}(\xi'_{0J} - \xi'_J)/\mathcal{E}^{(-1)}$ (see equation (10)) and, counting the number of fringes displaced, we could determine the disturbances present. In the bottom right corner of the image of figure 3(*b*) the fringes are straight,indicating that there is no disturbance, while in the top left corner the fringes are distorted because of fluctuations in the optical thickness of the Mylar and these can be determined using equation (10). However, in our experiment, the overall thickness of Mylar cannot be determined unequivocally since the strip is so thick and has been cut so sharply that the fringes in the neighbourhood of the border cannot be followed and there is an uncertainty in the wavefront deformation of an integer number of wavelengths. On the contrary, in figures 3(*a*), (*c*) and (*d*) the localization planes viewed do not coincide with the face of the plate containing the strip so the wavefronts emerging from the various source points are not distorted in the same region or in a similar way. The fringes seen in the top left corner are almost straight and the interferograms yield practically no information concerning the fluctuations in optical thickness of the Mylar while, since the Mylar is thick, in the region surrounding the border of the strip, the fringes depart from straightness, indicating that the wavefronts are distorted and vary their shape as they propagate and, also, that the localization depth (see equation (7)) is large.

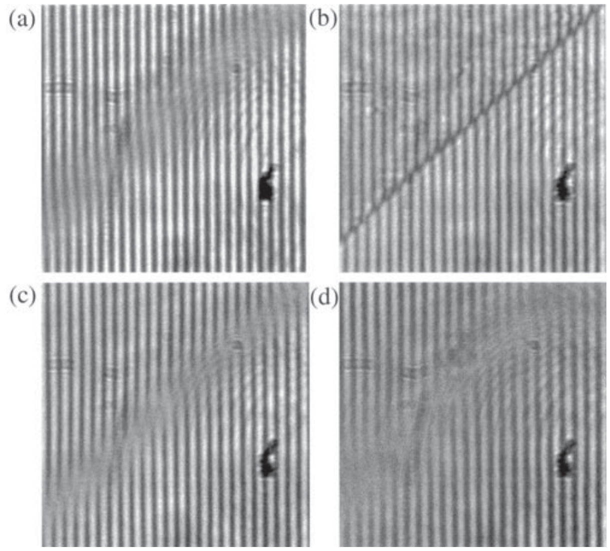

Figure 3. Images corresponding to (*a*) $\Sigma'_{-1}|_6$ (with $\delta x_6 = 0.130$ mm), (*b*) $\Sigma'_{-1}|_4$ (with $\delta x_4 = 0.174$ mm), (*c*) $\Sigma'_{-1}|_2$ (with $\delta x_2 = 0.217$ mm) and (*d*) Σ'_0.

3.2. Experiment 2: both faces of the specimen have disturbances

The glass plate has Mylar strips, approximately perpendicular to one another, adhered to both faces and is placed in the test arm with the strips forming approximately 45° with the fringes. We focus the observation system on the front face of the specimen, and choose a grating which yields the localization plane of order $m = -1$ on this face, then, without moving the specimen, we focus the rear face and change the grating to shift plane Σ'_{-1} and we obtain the images of figure 4. As expected, the variations of phase distort the fringes and the localization plane must coincide with the layer under test to enable the determination of its disturbances. In our experiment, however, the measurement is complicated because, owing to the large localization depth, when one face is focused, the disturbance on the other face is out of focus but also seen. This inconvenience could be overcome by diminishing the localization depth. According to equation (7), $\mathrm{LD}^{+}|_m$ depends on $F' + Z''_m$, $\varepsilon^{(m)}$ and 2; H and q_1, so to diminish $\mathrm{LD}^{+}|_m$ without increasing the source size we could, for example, reduce the distance $F' + Z''_m$. Moreover, in figure 4(*a*) the border of the strip

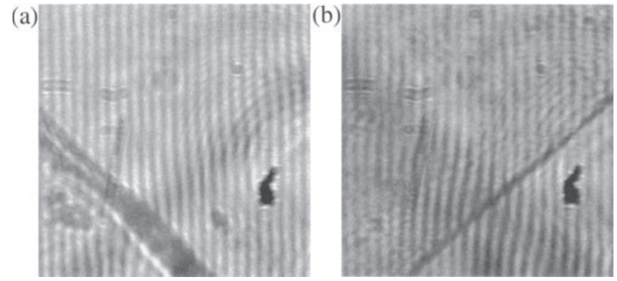

Figure 4. Images on both faces of a specimen when each of them coincides with the localization plane of order $m = -1$ corresponding to a grating of adequate period.

which is seen focused has been torn, generating a continuous deformation of the fringes in its neighbourhood; the overall thickness of the strip can be estimated and it is approximately $3\bar{\lambda}$. In contrast in figure 4(b) the border of the strip which is focused has been abruptly cut, the number of fringes present in the dislocation cannot be seen in detail, the phase shifts are not adequately resolved and the overall thickness of the Mylar cannot be determined unequivocally.

4. Discussion

The feasibility of testing a volume using a conventional Mach–Zehnder interferometer can be highly improved by illuminating it with a quasi-monochromatic, incoherent and periodic source of variable period since the inconvenience of either having to readjust the interferometer or displace the specimen is overcome. Leaving the phase object in a fixed position and without readjusting the device, defects present in different layers can be detected by shifting the localization plane by a change in the source period. However to calculate the amount of deformation present, the specimen has the limitations that the analysed layers must be optically continuous or with disturbances which are known to be smaller than the wavelength. The localization depth plays an important role in the degree of difficulty in interpreting the interferograms corresponding to different layers. A reduction of the localization depth could render better qualitative results and could be achieved by diminishing the distance between the plane containing the two images of the source through the interferometer and the localization plane.

Acknowledgments

The authors acknowledge the support of CONICET and Subsidio de UBA in developing this work. We are grateful to Mr Jan Hinnerk Scheel for his collaboration in the acquisition of the images and to Mr Ezequiel Carbón for drawing the figures.

Appendix. Alignment of the Mach–Zehnder interferometer

For the Mach–Zehnder to be aligned, the rays originating in the division of one incident ray must not be skew. The procedure of alignment has been explained in a previous paper [14] (we point out that due to an editing error in that paper the orders indicated on the right of figure 3 [14] are mistaken and from top to bottom they should be 2, 1, 0, −1, −2, −3 and −4). This procedure consists of the five following steps, each linked to a requirement.

Step 1. One ray emerging from the central source point splits in the interferometer into two rays which must not be skew and the fringe spacing can have a desired value. A polarized laser is used as an illumination system in such a way that the beam incident on the interferometer is linearly polarized perpendicular to its plane and, neglecting the angular spread, it is collimated and travels along the direction denoted z in figure 2(a). Each ray constituting the beam splits into two rays, which must remain in the same plane in order to interfere. To facilitate this alignment (though it is not necessary), the optical elements are placed in such a way that the beams are parallel to the table throughout, i.e. the z-axis is parallel to the table where the interferometer is mounted. When this alignment is achieved, the rays originating in the division of the ray along z, termed '$\mathrm{I_o}$' and '$\mathrm{II_o}$', intersect at a point $P'_{\mathrm{loc,o}}$ and form a bifurcation angle Λ'_{o}. Focusing $P'_{\mathrm{loc,o}}$ with a microscope objective, the superposition of the two beams is amplified and projected on a screen, fringes are seen and Λ'_{o} is modified by adjusting the interferometer until the fringe spacing, $\varepsilon^{(0)} = \bar{\lambda}/|\Lambda'_{\mathrm{o}}|$, has the desired value. Furthermore, on a screen placed approximately perpendicular to rays '$\mathrm{I_o}$' and '$\mathrm{II_o}$', one dot is seen if it coincides with the plane containing $P'_{\mathrm{loc,o}}$ and two dots if it is withdrawn from $P'_{\mathrm{loc,o}}$, so, measuring the distances between this position and $P'_{\mathrm{loc,o}}$ and between the two dots, Λ'_{o} is determined.

Step 2. A fan of rays emerging from the central source point splits in the interferometer giving rise to two fans, which must not be skew, and the position of the localization planes can be roughly estimated by considering the intersections of these fans. The illumination system is a Ronchi grating of period δx illuminated by the non-expanded laser beam of the previous step (which has a diameter greater than δx). For simplicity (though it is not necessary), we assume that the grating plane is perpendicular to the beam and this plane is termed (x, y) (with y parallel to the slits). The well known diffracted beams of different orders j (with j integer) emerge from the grating and corresponding diffraction orders, termed j' and j'', emerge from its images, σ' and σ''. Because of the adjustment of step 1, the order $j = 0$ is along z and the orders $j' = 0$ and $j'' = 0$ are in the direction of rays '$\mathrm{I_o}$' and '$\mathrm{II_o}$', which intersect at $P'_{\mathrm{loc,o}}$. However a whole fan emerging from the central point O, containing the diffraction orders and lying on the plane (x, z), can give rise to fans emerging from O′ and O″ that are skew and, in this case, the classical localization plane Σ'_0 does not exist. The interferometer is adjusted to roughly control that these two fans belong to the same plane by placing a screen approximately perpendicular to rays '$\mathrm{I_o}$' and '$\mathrm{II_o}$' and taking into account the two corresponding series of dots that are seen. When all the dots are aligned, the situation is that of figure 5(a), so if the screen is displaced, let us say from left to right, there are certain positions where the dots from σ' (indicated with small full circles) are seen superposed on those from σ'' (indicated with open circles) separated by regions where they are not superposed. This behaviour can be interpreted as follows. A ray from O of order j splits into two rays, which intersect at a point of the classical localization plane, i.e. at Σ'_0 the order $j'' = j$ is superposed on the order $j' = j$, and when the screen is placed at Σ'_0 the dots corresponding to the beams from σ' and σ'' are seen to coincide. If the alignment is correct, as the screen is displaced to the right (or left) of Σ'_0, the dots corresponding to σ' and σ'' begin to withdraw from one another until the order $j'' = j$ coincides with $j' = j + 1$ (or $j' = j - 1$), then the dots again withdraw from one another until that corresponding to $j'' = j$ coincides with that corresponding to $j' = j + 2$ (or $j' = j - 2$) and so on. For a point P$'$ of the observation space where the order $j' = j + m$ is superposed on the order $j'' = j$, in the source space there are corresponding rays from O, one of order $j + m$ and considered to travel through arm I and the other of order j and considered to travel through arm II (see figure 5(*b*)). Taking into account a source point, $S_{\delta x}$, a distance δx away from O, in arm II we consider ray OP_{II} and a parallel to it passing through $S_{\delta x}$, we draw the perpendicular $H_{II}P_{II}$ and we have $S_{\delta x}H_{II}/S_{\delta x}P_{II} = \cos\alpha_{II} \approx 1$ since, as is usual in the Mach–Zehnder, $\delta x \ll OP_{II}$ and the angle α_{II} between $S_{\delta x}H_{II}$ and $S_{\delta x}P_{II}$ is small. The ray of order j is part of the beam verifying that the difference in optical pathlength between light emerging from two successive grooves is $j\bar{\lambda}$, so

$$[OP_{II}] - [S_{\delta x}P_{II}] \approx [OP_{II}] - [S_{\delta x}H_{II}] = j\bar{\lambda}. \qquad \text{(A. 1)}$$

With similar considerations for arm I we obtain $[OP_{I}] - [S_{\delta x}P_{I}] \approx (j + m)\bar{\lambda}$. Thus the variation of optical pathlength difference from O and from $S_{\delta x}$ to point P$'$ (see equation (1)) is

$$\mathrm{VOPD}(P')|_{\delta x} = [S_{\delta x}P_{I}] - [S_{\delta x}P_{II}] - [OP_{I}] + [OP_{II}] \approx -m\bar{\lambda} \qquad \text{(A. 2)}$$

which is almost the condition that must be satisfied by the points of the planes Σ'_m (see equation (4)). Therefore the planes where the dots originating at σ' and σ'' are seen superposed are, approximately, the planes Σ'_m and the determination of their position yields a rough estimation of the positions of the localization planes. However since our intention is to use an extended source sufficiently large to assure a small localization depth, this adjustment is not sufficient to guarantee an adequate contrast at the localization surfaces.

Step 3. A fan emerging from any source point gives rise to a pair of fans which must not be skew and the contrast at the classical localization surface must be adequate. The illumination system is a moving point source obtained by replacing the grating by a microscope objective placed on a support which allows for fine movements. Since the source is a point, the only localization plane is Σ'_0, and when the alignment is adequate the fringes do not vary as the point source is displaced. Because of the adjustment of step 2, the fan originating at O and lying on the plane (x, z) gives rise to two fans, emerging from O$'$ and O$''$, which are also on this plane, and the same holds for the source points in the neighbourhood of O. However, this condition of coplanarity must be valid for any source point, even if it is not so close to O, so, moving the point source, we adjust the interferometer to achieve this.

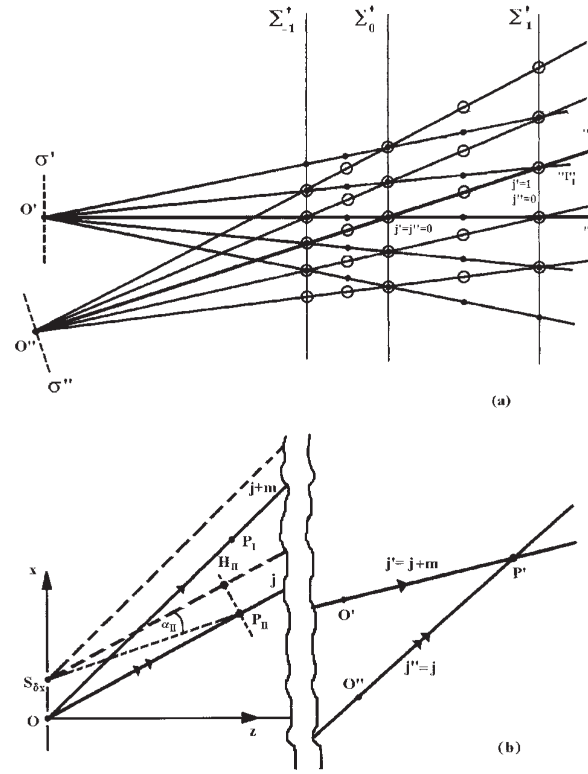

Figure 5. Alignment of the Mach–Zehnder when a non-expanded laser beam illuminates a grating of period δx. (*a*) σ' and σ'', images of the grating through both arms; open circles indicate rays of different orders j'' originating at O$''$; small full circles indicate rays of orders j' originating at O$'$. (*b*) P_I and P_{II}, images of P$'$ back through both arms; OP_{II} (and OP_I), ray of order j (and $j + m$); $S_{\delta x}$, point at a distance δx from O; $S_{\delta x}H_{II}$, parallel to OP_{II}.

Step 4. A small periodic source must yield localization planes of adequate contrast. The microscope objective is replaced by the grating of period δx, i.e. the illumination system is that of step 2. We perform fine adjustments to enable the interferometer to yield adequate contrast not only at Σ'_0 but also at any other localization plane.

Step 5. When the source is extended, incoherent and periodic, an adequate contrast must be encountered in the localization planes. The illumination system is an incoherent periodic source obtained by interposing a microscope objective, a condenser and a rotating diffusor between the laser and the grating. We use the observation system of figure 2(*b*) to see the interferograms on the video monitor and we perform the final adjustments to attain an adequate contrast on the localization surfaces.

References

[1] Steel W H 1967 *Interferometry* (London: Cambridge University Press)
[2] Malacara D 1978 *Optical Shop Testing* (New York: Wiley)
[3] Hariharan P 1969 Modified Mach–Zehnder interferometer *Appl. Opt.* **8** 1925–6
[4] Simon J M and Iemmi C C 1990 Interferometers: equivalent sine condition and pseudoholographic properties *Appl. Opt.* **29** 1868–9

[5] Schwider J and Falkenstrfer O 1995 Twyman–Green interferometer for testing microspheres *Opt. Eng.* **34** 2972–5

[6] Simon J M and Comastri S A 1980 Localization of interference fringes *Am. J. Phys.* **48** 665–8

[7] Simon J M and Comastri S A 1987 Fringe localization depth *Appl. Opt.* **26** 5125–9

[8] Simon J M and Comastri S A 1988 Interferometers: equivalent sine condition *Appl. Opt.* **27** 4725–30

[9] Simon J M, Simon M C, Echarri R M and Garea M T 1998 Fringe localization in interferometers illuminated by a succession of incoherent line sources *J. Mod. Opt.* **45** 2245–54

[10] Comastri S A, Simon J M and Tardin C 2000 Multilocalization and van Cittert–Zernike theorem 1. Theory *J. Opt. Soc. Am.* A **17** 1265–76

[11] Simon J M, Comastri S A and Tardin C 2000 Multilocalization and van Cittert–Zernike theorem 2. Application to the Wollaston prism *J. Opt. Soc. Am.* A **17** 1277–83

[12] Jahns J and Lohmann A W 1979 The Lau effect (a diffraction experiment with incoherent illumination) *Opt. Commun.* **28** 263–7

[13] Simon J M, Comastri S A and Echarri R M 2000 Shifting of localization planes in optical testing: application to a shearing interferometer *Cuaderno de Optica* **77** E Ediciones Previas, Lab. de Optica, FCEN-UBA, available from the authors at the address on the title page

[14] Simon J M, Echarri R M and Walsh P A 2000 Multilocalization of interference fringes in the Mach–Zehnder interferometer *Optik* **111** 307–9

[15] Malacara D, Serven M and Malacara Z 1998 *Interferogram Analysis for Optical Testing* (New York: Dekker)

[16] Dorredo B V and Fernandez J L 1999 Phase-evaluation methods in whole-field optical measurements techniques *Meas. Sci. Technol.* **10** 33–55